ISTITUTO NAZIONALE DI FISICA NUCLEARE

Sezione di Genova

INFN/TC-83/20
19 Dicembre 1983

P. Fernandes and R. Parodi: THERMAL BEHAVIOR OF HIGH FREQUENCY He II COOLED Nb CAVITIES WITH DEFECT FREE INTERNAL SURFACE.

Servizio Documentazione
dei Laboratori Nazionali di Frascati

Istituto Nazionale di Fisica Nucleare
Sezione di Genova

INFN/TC-83/20
19 Dicembre 1983

THERMAL BEHAVIOR OF HIGH FREQUENCY He II COOLED Nb CAVITIES WITH DEFECT FREE INTERNAL SURFACE(*)

P. Fernandes
Istituto per la Matematica Applicata del CNR, Genova

and

R. Parodi
INFN - Sezione di Genova, Genova

ABSTRACT

The thermal behavior of Nb superconducting resonant cavities cooled by a superfluid helium bath is simulated by the numerical solution of a mathematical model of heat generation and transfer in the cavity wall. The simulations results are compared with experimental data reported in the literature and a good agreement is found for cavities working above nearly 4 GHz. How the maximum attainable surface magnetic field and general features of the thermal behavior depend on some cavity parameters in the simulations results is also discussed.

1. - INTRODUCTION

Thermal breakdown is one of the phenomena limiting the field strength achievable in superconducting resonant cavities. It takes place when by increasing the field a critical temperature is reached because of dissipation for which the superconducting material comes back to its normal state. Even though other phenomena (i. e. multipacting and non resonant electron loading) can limit the field strength at a lower lev

(*) - Submitted to Cryogenics.

el, thermal breakdown seems to be the main problem in superconducting cavities working at frequencies above some GHz (4 GHz typically). Hence the growing interest in the models for the thermal behavior of superconducting cavities.

In the present paper we confine ourselves to the most favourable case of cavities with defect free internal surface (i. e. with uniform residual resistance); thus our computed values of the maximum surface magnetic field attainable have to be regarded as upper bounds since the practical values can be lower because of possible surface defects. The more our hypothesis of uniform residual resistance will be satisfied, the more the practical value will be close to the theoretical upper bound.

In Section 2 of this paper we propose a model for cavities thermal behavior; the model above is used in Section 3 to discuss how thermal behavior itself depends on some parameters and results following from it are checked in Section 4 for agreement with the experimental data reported in the literature.

2. - THE MODEL

Models for the thermal behavior of defect free superconducting cavities have been already reported in the literature[1, 2, 9]. Most of them however do not take into account neither the frequency dependence of the surface resistance nor the temperature dependence of the thermal conductivity; moreover the Kapitza resistance is often either fully[1] or partially[2] neglected. On the contrary in our model all the aforementioned phenomena are completely taken into account whereas the lateral heat flow has been still neglected as before. Although in reference (9) a similarly complete model for the defect free case is proposed only a few results are reported for that case as that paper is mostly devoted to defects behavior. Below we describe in full details our model.

2. 1. - Heat generation at the cavity internal surface

The surface resistance R_S of Nb is

$$R_S = R_{res} + R_{BCS} \tag{1}$$

where R_{res} is a temperature independent term referred to as residual resistance and R_{BCS} is the temperature dependent term explained by BCS theory of superconductivity. R_{res} is computed from the low field unloaded quality factor Q_o^{lf} under the hypothesis of uniform residual resistance (i. e. defect free surface) as

$$R_{res} = \frac{G}{Q_o^{lf}} - R_{BCS} \tag{2}$$

where G is the geometrical factor of the cavity

$$G = \omega \mu_o \frac{\int_v H^2 dV}{\int_s H_{||}^2 dS} \quad .$$

The BCS term is given by

$$R_{BCS} = A \frac{f^{\alpha}}{T_I} \exp\left(- \frac{\Delta}{K_B T_{CO}} \frac{T_{CO}}{T_I}\right) \tag{3}$$

where T_I is the internal surface temperature, f is the cavity frequency and, following Halbritter[3], we use the Nb typical values below

$$A = 4.01 \times 10^{-23} \frac{\Omega^{o}K}{Hz^{\alpha}} , \qquad \frac{\Delta}{K_B T_{CO}} = 1.85 , \qquad T_{CO} = 9.25^{o}K$$

$\alpha = 2$ below 5 GHz, $\alpha = 1.6$ above 12 GHz, $1.6 < \alpha < 2$ (linearly interpolated) between 5 and 12 GHz.

Equation (3) holds until T_I stays below the critical temperature T_c which we take as

$$T_c = T_{CO} \sqrt{1 - \frac{B}{B_c}} \tag{4}$$

where B is the surface magnetic field strength and $B_c = 2000$ G. When T_c is exceeded breakdown takes place. From the surface resistance the heat flow density at the internal surface q_I is computed as

$$q_I = \frac{1}{2\mu_o^2} R_S(T_I) B^2 \tag{5}$$

where μ_o is the permeability of vacuum.

2. 2. - Heat conduction in the cavity wall

From a strict view-point the problem of the heat conduction in the cavity wall should be solved in three dimensions (or two if cylindrical symmetry holds) because B and thus q_I change from point to point along the internal surface. However we are only interested in the region of the surface where the maximum value of B occurs as it is the behavior of that region which ultimately sets the limit to the cavity performances. Thus, since as a general rule B changes weakly near its greatest value, we

do small errors if we solve the problem as one-dimensional by taking into account the normal heat flow only(x).

To deal with the local shape of the wall at the point where B takes its maximum value we transform the heat flow equation $\vec{\nabla}\cdot(K\vec{\nabla}T) = 0$ to suitable coordinates systems before reducing it to one-dimensional. This process leads us to the equation

$$\frac{d}{dx}\left(K\,\frac{dT}{dx}\right) = 0 \qquad (6)$$

for a plane wall and to the equation

$$\frac{d}{dr}\left(K\,\frac{dT}{dr}\right) + \frac{K}{r}\,\frac{dT}{dr} = 0 \qquad (7)$$

for a cylindrical wall. For a more general shape besides the curvature due to the cylindrical symmetry as in equation (7) we take into account also the local slope and curvature along the cavity axis; this yields more complex equations that we do not report.

For the thermal conductivity we use experimental data concerning our niobium(15). This makes nonlinear all the equations above and rules out closed form solutions for them. The thermal conductivity curve of our niobium (RRR = 62) is shown in Fig. 1. Notice that this curve agrees very well with the general shape predicted by the Wiedemann-Franz law and with the curves reported in the literature(10) for niobium with similar RRR.

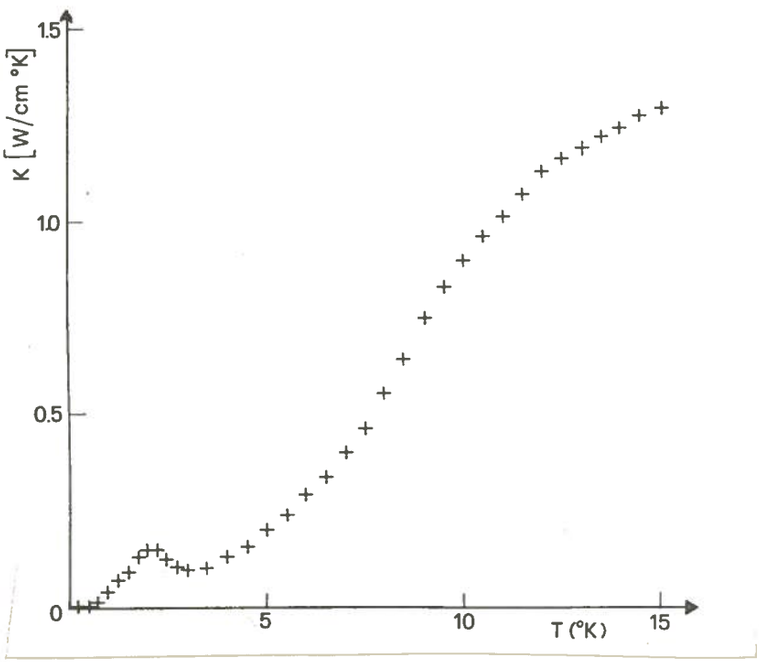

FIG. 1 - Measured thermal conductivity of Nb used in the model (RRR = 62).

(x) - The claim above is confirmed also by the results of Isagawa calculations(2).

2. 3. - Kapitza resistance and He II film boiling

To deal with the Kapitza resistance which develops at the Nb/He II interface we compute the temperature T_E of the cavity external surface as

$$T_E = (T_B^4 + 4 R_K q_E T_B^3)^{1/4} \tag{8}$$

where R_K is the Kapitza resistance, q_E the heat flow at the external surface and T_B the He II bath temperature. Equation (8) is the same as the more customary writing

$$R_K q_E = \Delta T \left[1 + \frac{3}{2} \frac{\Delta T}{T_B} + \left(\frac{\Delta T}{T_B} \right)^2 + \frac{1}{4} \left(\frac{\Delta T}{T_B} \right)^3 \right] \tag{9}$$

(where $\Delta T = T_E - T_B$) with all its terms kept. For Kapitza resistance value Mittag[4] reports

$$R_K^{-1} = (0.020 \pm 0.003) \times 10^4 \; T^{(4.65 \pm 0.28)} \; \frac{W}{m^2 {}^oK} \tag{10}$$

for chemically polished, annealed and again chemically polished Nb and

$$R_K^{-1} = (0.017 \pm 0.002) \times 10^4 \; T^{(3.62 \pm 0.32)} \; \frac{W}{m^2 {}^oK} \tag{11}$$

for machined Nb. We always use equation (10) except for cavities that underwent a very poor surface treatment like a light chemical polishing (10-30 μm) after machining without any heat treatment.

Equation (8) holds below a critical heat flux at which He II film boiling starts and thus the heat transfer coefficient sharply decreases by approximately one order of magnitude. When this happens breakdown immediately follows. Experimental data for the He II critical heat flux show a rather large scattering and are influenced by the geometry and the submersion depth of the specimen and by the temperature and the subcooling of the He II; so we have preferred that the film boiling was not simulated in the computer implementation of the model and thus the results have to be discussed taking into account this fact. To this purpose, in agreement with the rather scarce data for large specimens (not thin wires) in near saturated He II[5, 6, 7] we assume a critical heat flux somewhere in the range 2-4 W/cm^2. The often assumed value of 1 W/cm^2 refers to He II constrained in a long tube and is in our opinion too conservative. Our estimation could still be a conservative one because critical fluxes above 6 W/cm^2 have been observed[6].

2.4. - The mathematical problem

By putting together the above equations a two point boundary value problem is obtained that, to be specific, we write for the case of the cylindrical wall:

$$\begin{cases} \dfrac{d}{dr}\left(K(T)\,\dfrac{dT}{dr}\right) + \dfrac{K(T)}{r}\,\dfrac{dT}{dr} = 0 & (12) \\ -K(T_I)\,\left.\dfrac{dT}{dr}\right|_{r=r_I} = \varphi(T_I, B) & (13) \\ T_E = \psi\left(-K(T_E)\,\left.\dfrac{dT}{dr}\right|_{r=r_I}\right) & (14) \end{cases}$$

where r_I and r_E are respectively the internal and the external radius of the wall, $T_I = T(r_I)$, $T_E = T(r_E)$,

$$\varphi(T,B) = \frac{B^2}{2\mu_o^2}\left(R_{res} + A\,\frac{f^\alpha}{T}\,\exp\left(-\frac{\Delta}{K_B T_c}\,\frac{T_c}{T}\right)\right) \qquad (15)$$

and

$$\psi(q) = \left(T_B^4 + 4R_K q\,T_B^3\right)^{1/4}. \qquad (16)$$

We do not report here about the numerical method used by us to solve this problem as we have published it elsewhere[8]. By solving the above problem for several values of B we obtain a few interesting curves (e.g. T_I versus B) and the greatest B value attainable before reaching the superconductivity break down for a given set of physical cavity parameters (R_{res}, wall thickness, operating temperature, thermal conductivity, ...).

3. - QUALITATIVE RESULTS BY THE MODEL

The curves $T_I(B)$, $R_S(B)$ and $q_E(B)$ obtained by simulating the same cavity (4.5 GHz, 2 mm thick) with three different values of R_{res} (i.e. $3\times10^{-6}\ \Omega$, $10^{-6}\Omega$ and $2.5\times10^{-7}\ \Omega$) are shown in Figs. 2-4. These curves do not account for the possible getting over of either the critical heat flux or the critical temperature but the limits beyond of which they no longer make sense are drawn in the same figures. The (a), (b) and (c) curves are representative of the typical qualitatively different thermal behaviors which may occur at frequencies above some GHz. The (a) curves show a smooth decreasing of the cavity performances (thermal run-away) which makes it already unusable before the breakdown takes place because critical temperature or

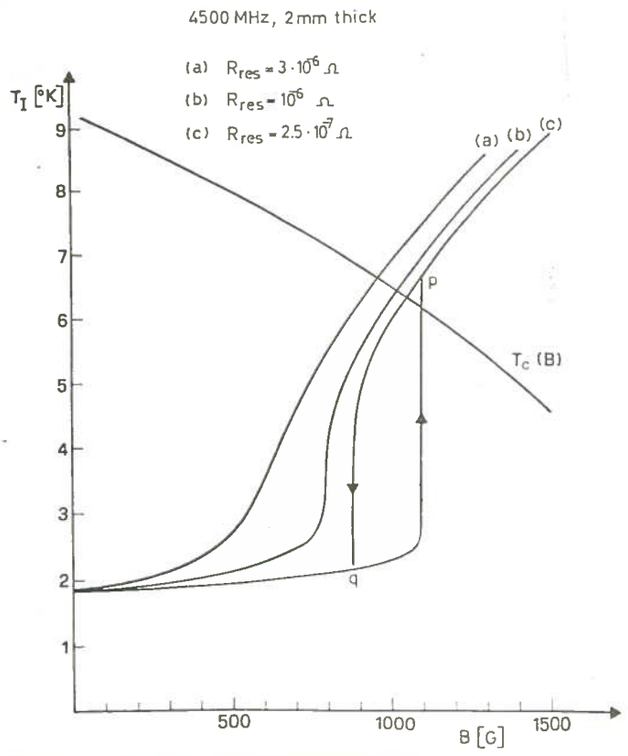

FIG. 2 - Internal surface temperature versus surface magnetic field as obtained by the model.

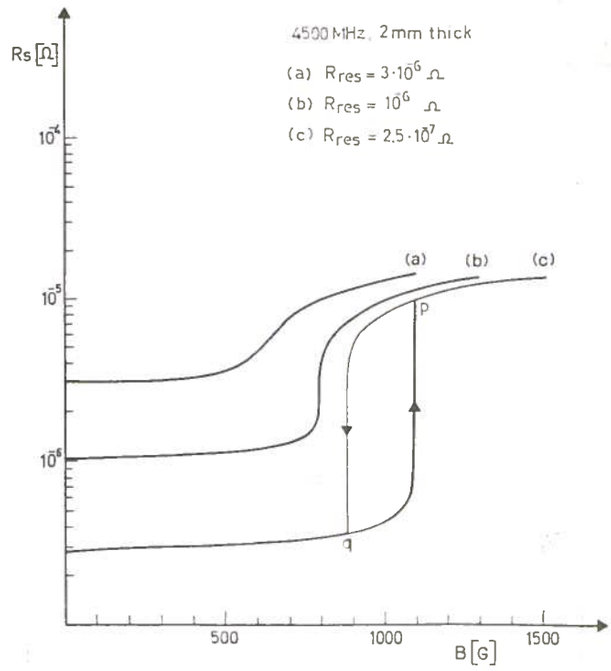

FIG. 3 - Surface resistance versus surface magnetic field as obtained by the model.

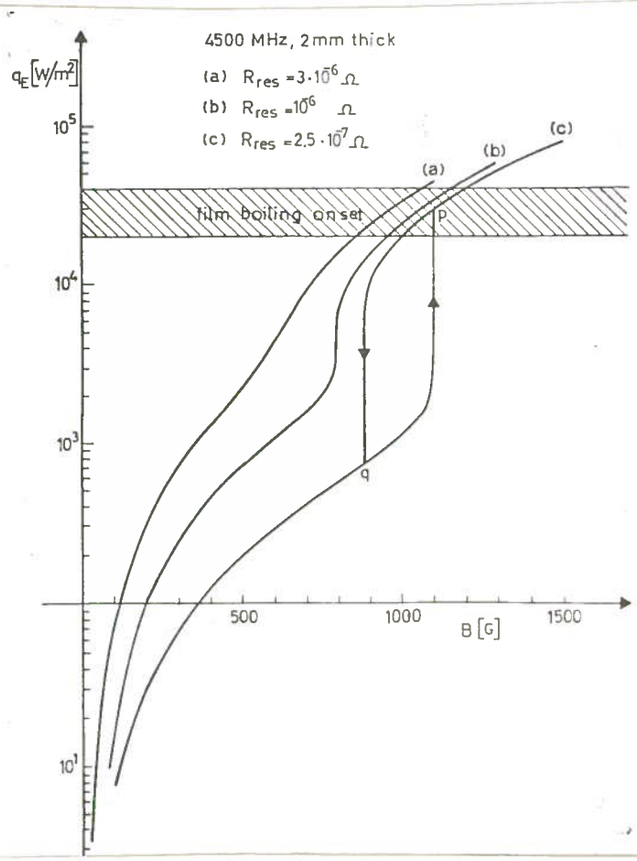

FIG. 4 - External surface heat flow versus surface magnetic field as obtained by the model.

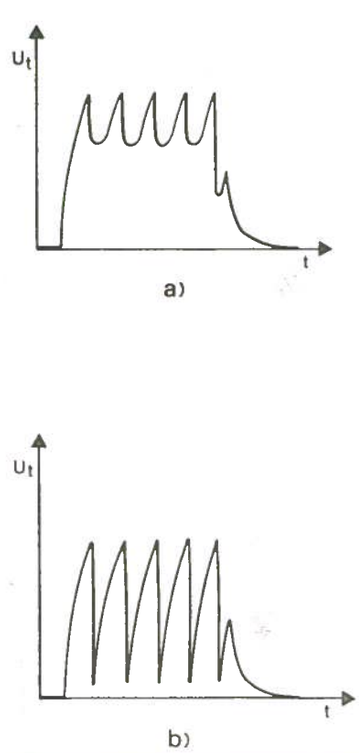

FIG. 5 - Transmitted power signals: (a) thermal instability without breakdown; (b) breakdown.

heat flux are exceeded, the real limitations being the power available and that which the refrigeration system allows to dissipate. The B value at which the thermal run-away begins is not sharply defined but can be fairly easily found on the $R_S(B)$ curve (roughly 500 G in our case).

In the (b) and (c) cases there is a critical value B_c^{th} of the magnetic field at which the temperature rises sharply (thermal instability) and the cavity quality factor greatly degradates. If in the new point of thermal equilibrium that the cavity would reach after the thermal instability either the critical heat flux or the critical temperature are exceeded, the breakdown takes place and our curves no longer make sense; otherwise the cavity still keeps superconducting though at higher temperature and dissipation. It is difficult to connect the simulation results for the steady-state thermal behavior directly to the observed RF signals, but this sudden quality factor degradation without breakdown seems to be qualitatively consistent with transmitted power signals as in Fig. 5a whilst breakdown seems consistent with signals as in Fig. 5b.

However in cases like (b) and (c) both if breakdown takes or does not take place it is the thermal instability which sets the limit for the practically achievable magnetic field. In principle there could be also the case in which T_I reaches T_c giving rise to the breakdown before thermal instability or run-away occur but this does not happen above some GHz for practical values of parameters (e.g. $R_{res} \simeq 3 \times 10^7 \Omega$ or Q_o^{lf} 10^9). On the contrary this is the usual case at lower frequencies where, however, the model does not fit experimental data as we will say in the next Section. In the reported example the thermal instability causes the breakdown in the (c) case whereas in the (b) case does not produce it; this is a quite typical case but there are also cases of (c) type in which the thermal instability does not trigger breakdown.

The reason for the previously described thermal instability can be found in the highly nonlinear temperature dependences of the surface and the Kapitza resistances which allow for the possibility that the heat produced at the cavity internal surface grows with the temperature more strongly than the heat conducted away to the helium bath. When, depending on parameters values, this happens the thermal instability takes place. The temperature dependence of the conductivity of the niobium plays a minor role as the thermal instability follows from the model also in cases for which a constant conductivity was assumed.

From our simulations we obtained also the following results concerning B_c^{th} above some GHz (below we will indicate by B_c^{th} also the not sharply defined value of the (a) case):

- An increase of the wall thickness always reduce B_c^{th} (see Fig. 6), changes the thermal behavior from (a) to (c) cases and increases the hysteresis amplitude in the (c) case.
- An increase of R_{res} always reduces B_c^{th} (see Fig. 6), decreases the hysteresis amplitude in the (c) case and changes the thermal behavior from (c) to (a) case.
- R_K acts in a similar ways as R_{res} but with less marked effects.
- There is a temperature of He II bath which gives the greatest B_c^{th}. This temperature decreases if we increase the wall thickness or R_K and shows a nearly insensible increasing with R_{res} (see Fig. 7).

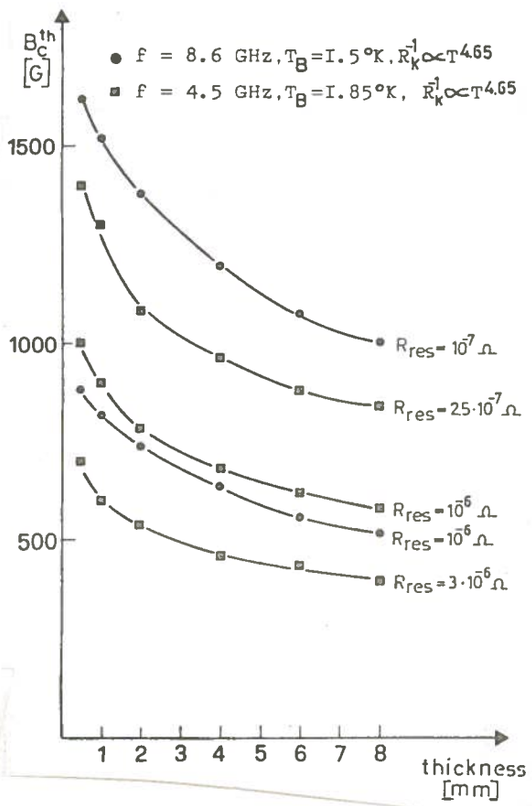

FIG. 6 - Maximum attainable magnetic field versus cavity wall thickness as obtained by the model.

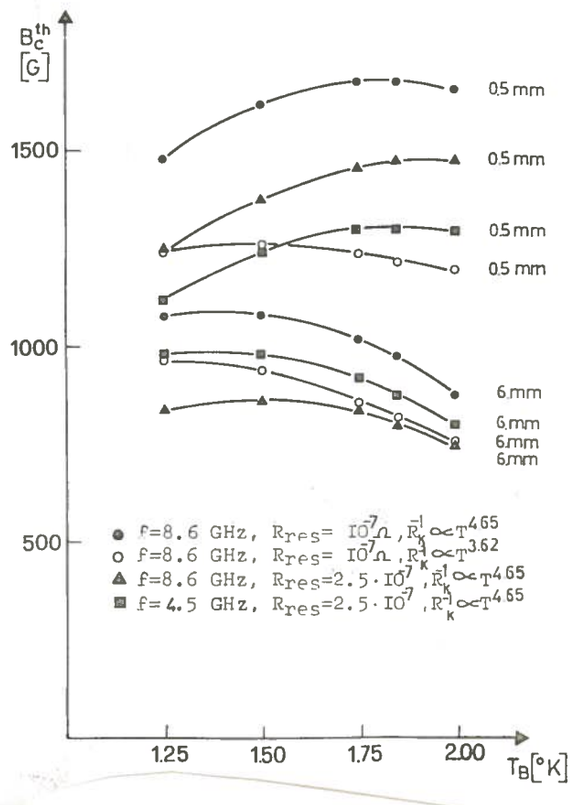

FIG. 7 - Maximum attainable magnetic field versus bath temperature as obtained by the model.

4. - COMPARISON BETWEEN RESULTS BY THE MODEL AND EXPERIMENTAL DATA

We have checked our model by using it to calculate the maximum B value in cavities for which experimental data are reported in the literature. The results are summarized below and their discussion follows.

In reference (11) experimental results for 4.5 GHz door-bell cavities were reported; for the best of them the quality factor at low field was 2.24×10^9 and the

breakdown occurred for a peak surface magnetic field of 1040 G. In the simulation with the same Q_o^{lf} ($R_{res} = 9.2 \times 10^{-8}\ \Omega$) the breakdown takes place, following a thermal instability, at a field level of 1360 G.

In reference (12) we reported experimental data for other 4.5 GHz door-bell cavities chiefly differing from the previous ones for the thickness of the niobium wall, the formers being 1 mm thick, the latters 2 mm. Two qualitatively different behaviors were observed in these 2 mm thick cavities: thermal run-away at about 300-350 G for $Q_o \simeq 10^8$ or sudden degradation of cavity performances at about 500-550 G (for $Q_o \simeq 3 \times 10^8$). In this latter case the transmitted power signals were as in Fig. 5a. The corresponding results of simulations are thermal run-away at about 500 G for the lowest Q_o value ($R_{res} = 3 \times 10^{-6}\ \Omega$) and thermal instability not followed by breakdown at about 750 G for the highest Q_o value ($R_{res} = 10^{-6}\ \Omega$).

The highest surface magnetic field obtained in 8.6 GHz muffin-in cavities for which experimental results are reported in reference (13) was 1600 G. Our model gives a breakdown due to thermal instability at field levels about 1700-1800 G. Since quoted reference does not report the precise Q_o value for this single cell best case the low field R_{res} values for the several simulations performed were estimated on the basis of a set of experimental Q_o values reported in the same reference for a multicell cavity.

In reference (14) Pfister reports the measured Q_o values of a 9.5 GHz anodized TE_{011} resonator as a function of the magnetic field. In order to utilize our model for anodized cavities we must take into account that two different values of $\Delta/K_B T_{CO}$ should be used in equation (3) for different ranges of temperature[3]. Thus we have fitted lower and higher field Pfister's data by using $\Delta/K_B T_{CO} = 1.55$ for $T_I < 1.55^oK$, $\Delta/K_B T_{CO} = 1.79$ for $T_I > 1.70^oK$ together with suitable R_{res} values. The resulting $Q_o(B)$ curves are shown in Fig. 8; another curve obtained by trying to fit the whole set of experimental points by a single intermediate $\Delta/K_B T_{CO}$ value is also shown in the same figure.

The peak surface magnetic field given by the model when the parameters are chosen to fit the higher field experimental points is 1600 G; the experimental one for the cavity to which Pfister's $Q_o(B)$ graph refers was about 1500 G but also a value of 1590 G is reported for another cavity of the same type.

As a first comment on the comparisons of the previous paragraphs let us notice that the model always gives peak surface magnetic field values higher than the experimental ones as it should be (see Section 1). Moreover these values are not too much higher than measured ones and the better the surface treatment a cavity received, the

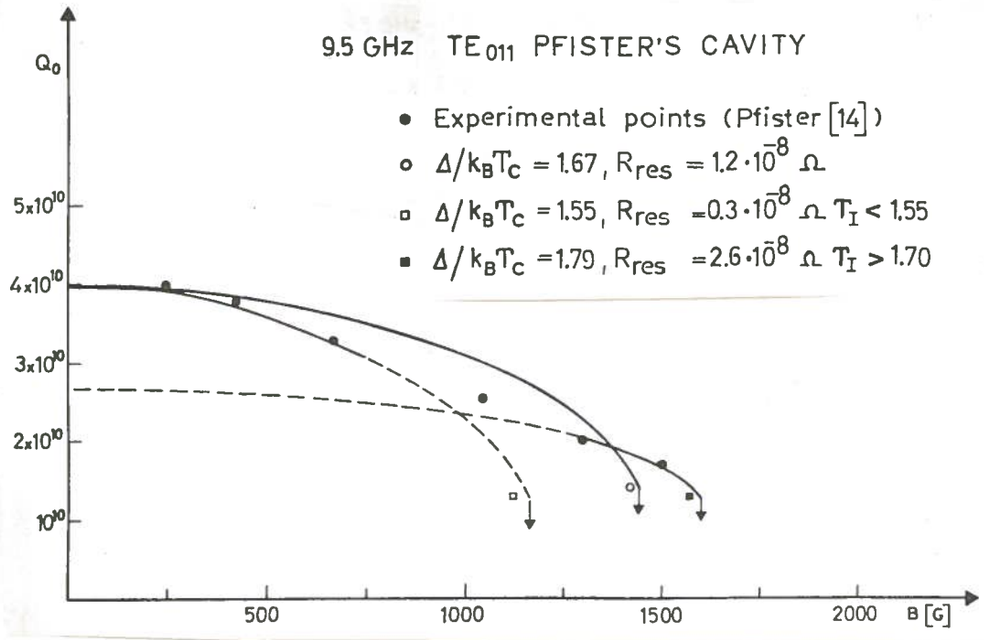

FIG. 8 - Model results fitting quality factor versus surface magnetic field experimental data by Pfister[14].

lesser is the difference between the measured peak field and its theoretical upper bound. This latter fact is not surprising since the better surface treatment, the more the hypothesis of uniform residual resistance is satisfied. The cavities of reference (12), in which a rather lower magnetic field was measured than the upper bound by the model, indeed received a very simple surface treatment allowing for a fairly variable residual resistance. On the other hand for the TE_{011} resonators of reference (14), which underwent a very careful surface treatment, experimental and computed values of maximum achievable B field are much closer and moreover a very good agreement is observed between measured and computed $Q_o(B)$ values from low field strengths to the thermal instability.

Finally let us say that any attempt to obtain useful results below 3 GHz proved unsuccessful as the field values by the model were always too much higher than the experimental ones. This fact was not completely unexpected as several reasons can be given for it. First of all at these frequencies the main problem is the electron loading and even if a thermal breakdown ultimately occurs the heat produced at the internal surface of the cavity by the impinging electrons plays a major role. Moreover the hypothesis of uniform residual resistance is not so good as at higher frequencies since (a) the aforesaid impinging electrons can also cause surface damages thus producing local defects of high R_{res}, (b) a larger internal surface entails a greater probability of surface defects and (c) the greater is the cavity the harder is to achieve an uniform surface treatment, which still implies an increasing of surface defects probability.

5. - CONCLUSIONS

In this paper we proposed a model of the thermal behavior of superfluid helium cooled niobium cavities with defect free internal surface. This model was checked by comparison with experimental data and a good agreement was obtained above nearly 4 GHz especially for cavities which underwent careful surface treatments producing a very uniform surface resistance. The qualitative results of Section 3 and numerical solutions of the model in particular cases should prove useful in designing superconducting cavities working above 4 GHz.

REFERENCES

(1) - B. Hillenbrand, H. Martens, H. Pfister, K. Schnitzke and G. Ziegler, IEEE Trans. on Magnetics MAG-11, 420 (1975).

(2) - S. Isagawa and K. Isagawa, Cryogenics 20, 677 (1980).

(3) - J. Halbritter, Proceedings of the Workshop on RF Superconductivity, Karlsruhe report KFK 3019 (1980), p. 190.

(4) - K. Mittag, Cryogenics 13, 94 (1973).

(5) - J. S. Goodling and R. K. Irey, Adv. Cryog. Eng. 14, 159 (1969).

(6) - D. N. Lyon, Intern. Adv. Cryog. Eng. 10, 371 (1965).

(7) - S. W. Van Sciver and R. L. Lee, Adv. Cryog. Eng. 25, 363 (1980).

(8) - P. Fernandes and R. Parodi, Report INFN/TC-83/10 (1983).

(9) - H. Padamsee, Report CERN/EF/RF 82-5 (1982).

(10) - Thermal conductivity of solids at room temperature and below, NBS Monograph 131 (1975), p. 53.

(11) - V. Lagomarsino, G. Manuzio, R. Parodi and R. Vaccarone, IEEE Trans. on Magnetics MAG-15, 25 (1979).

(12) - P. Fernandes, V. Lagomarsino, G. Manuzio, R. Parodi and R. Vaccarone, IEEE Trans. on Magnetics MAG-19, 1334 (1983).

(13) - H. Padamsee, M. Banner, J. Kirchgessner, M. Tigner and R. Sundelin, IEEE Trans. on Magnetics MAG-15, (1979), p. 602.

(14) - H. Pfister, Cryogenics 16, 17 (1976).

(15) - E. Massabò, Thesis Genoa University (1977).